

Accuracy of implementing principles of fusion imaging in the follow up and surveillance of complex aneurysm repair

Journal:	<i>Vascular Medicine</i>
Manuscript ID	VMJ-17-2840.R2
Manuscript Type:	Special Issue: Vascular Imaging/Diagnostics
Date Submitted by the Author:	29-Jan-2018
Complete List of Authors:	Martin-Gonzalez, Teresa; Royal Free London NHS Foundation Trust, Vascular Surgery Penney, Graeme; King's College London School of Medical Education, Engineering Chong, Debra; Royal Free London NHS Foundation Trust, Vascular Surgery Davis, Meryl; Royal Free Hospital, Royal Free London NHS Foundation Trust; Mastracci, Tara; Royal Free Hospital, Royal Free London NHS Foundation Trust
Keywords:	Abdominal Aortic Aneurysm (AAA), Endovascular Therapy, Vascular Imaging
Abstract:	<p>Fusion imaging is standard for the endovascular treatment of complex aortic aneurysms, but its role in follow-up has not been explored. A critical issue is renal function deterioration over time. Renal volume has been used as a marker of renal impairment, however it is not reproducible and remains a complex and resource-intensive procedure. The aim of this study is to determine the accuracy of a fusion-based software to automatically calculate the renal volume changes during follow-up. In this study, CT scans of 16 patients who underwent complex aortic endovascular repair were analysed. Preoperative, 1-month and 1-year follow-up CT scans have been analysed using a conventional approach of semiautomatic segmentation, and a second approach with automatic segmentation. For each kidney and at each time point the percentage of change in renal volume was calculated using both techniques. After review, volume assessment was feasible for all CT scans. For the left kidney, Interclass Correlation Coefficient (ICC) was 0.794 and 0.877 at 1-month and 1-year, respectively. For the right side, ICC was 0.817 at 1 month and 0.966 at 1 year. For the >60% scans, the automated technique reliably detected a decrease in renal volume for patients with occluded renal arteries during follow-up. This is the first report of a fusion-based algorithm to detect changes in renal volume during post operative surveillance using an automated process. Using this technique, the standardised assessment of renal volume could be implemented with greater ease and reproducibility and serve as a warning of potential renal impairment.</p>

1
2
3
4
5
6
7
8
9
10
11
12
13
14
15
16
17
18
19
20
21
22
23
24
25
26
27
28
29
30
31
32
33
34
35
36
37
38
39
40
41
42
43
44
45
46
47
48
49
50
51
52
53
54
55
56
57
58
59
60

SCHOLARONE™
Manuscripts

For Peer Review

1
2
3
4
5 1 Accuracy of implementing principles of fusion imaging in the follow
6
7 2 up and surveillance of complex aneurysm repair
8 3 Feasibility of
9 4 implementing principles of Fusion imaging in the Follow-up of
10 5 Complex Aneurysm Repair
11
12
13
14

15 T Martin-Gonzalez¹, G Penney², Chong D¹, M Davis¹, TM Mastracci¹

16
17 ¹Royal Free Hospital, London, UK

18
19 ²CYDAR imaging, Cambridge, UK/Imperial College, London, UK
20
21

22
23
24
25
26
27
28
29

30
31
32
33
34
35
36
37
38
39
40
41
42
43
44
45
46
47
48
49
50
51
52
53
54
55
56
57
58
59
60

9 Word Count: 2727

12 Corresponding Author,

13 TM Mastracci

14 Clinical Lead, Aortic Surgery

15 Royal Free London

16 Pond Street

17 London, UK

18 NW3 2QG

19 tara.mastracci@nhs.net.

1 Introduction

2 The endovascular treatment of complex aneurysm has evolved as an alternative to
3 open repair (1) and it has become standard of care in many jurisdictions. Although
4 outcomes are durable(2)(3)(4)(5), renal impairment during follow up is still a critical
5 issue, and difficult to quantify. Many different markers, such as renal volume, stent
6 angulation, and stent stenosis, have been used to predict renal impairment.-(6)(7)(4)
7 Using a combination of these variables is not a reproducible method to assess renal
8 impairment, despite being a complex and resource-intensive process.

9
10 Advanced imaging techniques such as 3D fusion significantly reduces radiation
11 exposure and contrast utilization in EVAR as well as in complex endovascular
12 procedures (8). However utilizing the principles of fusion ~~imaging~~ in follow-
13 up has not been explored. The aim of this study is to determine the accuracy of
14 fusion-based techniques to automatically calculate the renal volume changes during
15 follow-up with automated segmentation software, and standardise its use.

17 Material and Methods

18 *Study population.* We selected CT scans of 16 patients who went under complex
19 aortic endovascular repair in our centre to include in this analysis. This group
20 included 8 patients who underwent FEVAR with no complications throughout
21 follow-up, and 8 patients who sustained at least one renal occlusion during follow-up.
22 We assumed that renal occlusion would be the most dramatic event leading to renal
23 volume change. The patients were drawn from the local experience of cases performed
24 between 2012 and 2016. Inclusion required a renal event with at least one CT scan after
25 the event occurred. Controls were chosen to match patients with renal events.
26 Demographics of both are included in table I.

1
2
3 1
4
5 2 Retrospectively both preoperative, 1-month and 1-year follow-up CT scans were
6
7 3 analysed using a conventional approach of semiautomatic segmentation in
8
9 4 conventional software, and using a second approach exploring new software with
10
11 5 automatic segmentation. The rationale behind analysing serial images is to determine
12
13 6 the degree of accuracy this method has in assessing change in renal volume, as it is
14
15 7 well established that ~~devascularization~~devascularisation of a kidney leads to
16
17 8 progressive shrinkage of the kidney over time. Ethical approval of the local
18
19 9 institution was waived as this is a retrospective observational study.

20
21
22 10
23
24 11 *Renal function.* The eGFR was determined by the abbreviated MDRD study equation
25
26 12 (eGFR [ml x min⁻¹ x 1.73 m⁻²] = 186 x [serum creatinine]^{-1.154} x [age]^{-0.203} x [0.704 if
27
28 13 female] x [1.210 if African American]). The eGFR was calculated preoperatively, at
29
30 14 1 month and at 1-year follow-up.

31
32
33 15
34
35 16 *Imaging analysis.* Using the conventional system, CTs were interrogated using a
36
37 17 multiplanar three-dimensional workstation (AquariusNet software, TeraRecon Inc,
38
39 18 San Mateo, Calif). Renal events were agreed by two investigators. The volume of
40
41 19 each kidney was calculated with the following method: after selection of an area of
42
43 20 interest, a ~~semiautomated~~semi_automated post-processing algorithm extracted the
44
45 21 renal contour based on pixels of similar attenuation; the pelvicalyceal system, fat and
46
47 22 vessels in the renal sinus, and renal cysts were excluded by manual correction on
48
49 23 multiplanar views (to correct for any confounding automatic inclusion); finally, the
50
51 24 renal volume was estimated with an algorithm embedded in the software package (in
52
53 25 cubic centimetres) (Figure 1). The robustness of this method has been published in a

1
2
3 1 previous study (9). Predicted postoperative eGFR was calculated by renal volume
4
5 2 change using the equation developed by Shimoyama et al (10): *predicted*
6
7 3 *postoperative eGFR= preoperative eGFR x (postoperative renal volume/preoperative*
8
9 4 *renal volume)*. The correlation between the predicted and the observed postoperative
10
11 5 eGFR has been quantified.

12
13 6 An overview of the new fusion-based method is shown in [figure 2](#). The operator used
14
15 7 the itknap image viewer (www.itknap.org)(11) to manually select 6 points in the
16
17 8 preoperative CT and a single point in the postoperative CT. These points were used
18
19 9 to provide a starting position and region-of-interest for the automatic fusion
20
21 10 algorithm.

22
23
24
25 11 The algorithm then proceeds automatically and iteratively translates, rotates and
26
27 12 scales the postoperative CT and compares it with the preoperative image of the
28
29 13 kidney. The images are compared using a statistical measure (correlation coefficient)
30
31 14 applied to the underlying voxel intensity values. When an optimum fusion is achieved
32
33 15 the postoperative kidney will be positioned and scaled so it closely resembles the
34
35 16 preoperative kidney. The amount of scaling applied to fuse the images is a
36
37 17 measurement of change in kidney size – the scaling occurs automatically in two
38
39 18 dimensions and the degree of change is calculated by the programme. In the example
40
41 19 shown the algorithm increased the size of the postoperative kidney by a factor of 1.81
42
43 20 to accurately fuse with the preoperative kidney. Alternatively this could be stated as:
44
45 21 the postoperative kidney has shrunk to 55% (1/1.81) of its preoperative volume.

46
47 22 For each kidney and at each time point the percentage of change in renal volume
48
49 23 compared to the preoperative one has been calculated using both techniques and the
50
51 24 reliability of ratings has been assessed.

52
53
54
55
56
57
58
59
60 25

1
2
3 1 *Statistical analysis.* Statistical analysis was performed in SPSS version 20 (Statistical
4
5 2 Package Social Sciences Inc., Chicago, IL, USA). Descriptive statistics were
6
7 3 generated, and the correlation between predicted and observed eGFR was calculated
8
9 4 with the Pearson correlation. The reliability of ratings has been assessed with the
10
11 5 interclass correlation coefficient and the Pearson correlation. The test value was
12
13 6 defined as $p < 0.05$.
14
15
16
17

18 **Results**

19
20 9 Table 1 summarizes the demographic characteristics of the 16 patients included in the
21
22 10 study, divided by group. The median preoperative eGFR was 80.5 ml/min [49.25-
23
24 11 89.75] in the group without renal occlusion during follow up and 55 ml/min [42.25-
25
26 12 74.50] in the occlusion group. Renal volume assessment was feasible for all CT scans
27
28 13 included in the study. Correlation between predicted eGFR, based on renal volume
29
30 14 calculated with the ~~semiautomated~~semi automated process, and observed eGFR was
31
32 15 $r=0.844$ ($p < 0.000$) is depicted in figure 3. Divided into non-occlusion and occlusion
33
34 16 group, the correlation was $r=0.899$ ($p=0.001$) and $r=0.800$ ($p=0.031$) respectively.
35
36
37
38
39

40 18 We assessed the reliability of both analysis techniques using the Interclass Correlation
41
42 19 Coefficient (ICC). For the left kidney, the ~~Interclass Correlation Coefficient (ICC)~~
43
44 20 was 0.794 and 0.877 at 1-month and 1-year follow-up, respectively. For the right side,
45
46 21 at 1-month the ICC was 0.817 and 0.966 at 1-year. For each kidney and at each time
47
48 22 point, the Pearson correlation coefficient was 0.770, 0.811, 0.710 and 0.942
49
50 23 respectively. ~~Figure 4 shows the correlation for the right kidney at 1-year follow-up.~~
51
52 24 For a small number of kidneys (~5%) differences greater than 30% between
53
54
55
56
57
58
59
60

1
2
3 1 automated and semiautomatic methods were observed. Methods are being tested to
4
5 2 improve robustness and automatically detect these outliers.

6
7 3 Table 2 describes the ability of the automated technique to ~~reliably~~ detect a decrease
8
9 4 in renal volume for patients with occluded renal arteries when preoperative imaging is
10
11 5 compared with the moment of detecting renal occlusion.
12
13 6

14 15 16 7 **Discussion**

17
18 8 In this study we demonstrate the accuracy of fusion-based software to automatically
19
20 9 detect and calculate renal volume changes during follow-up after aortic endovascular
21
22 10 repair. Using the established, reproducible, semi-automated technique to calculate
23
24 11 renal volume (9), we have calculated renal volume in a sample of 16 patients. Using a
25
26 12 process involving fusion techniques, we were able to assess the automated detection
27
28 13 of renal volume and calculation of volume changes in CT images gained throughout
29
30 14 the surveillance period. In addition, comparing patients with and without any renal
31
32 15 changes, the automated detection accurately ascertained the presence of renal volume
33
34 16 both with and without contrast, and identified renal artery occlusion accurately. We
35
36 17 believe this new technique may provide a robust, timely and reliable method for
37
38 18 advanced analysis of postoperative surveillance studies; thereby a more accurate
39
40 19 assessment can be performed in routine practice outside of investigational protocols.
41
42 20

43
44
45
46 21 As shown in different studies, renal volume is a reproducible and valid marker of
47
48 22 renal impairment when decreased blood supply or anatomic causes for renal
49
50 23 impairment are present. Renal volume has been assessed in various urologic studies as
51
52 24 a predictor of graft function in living donor transplantation (12)(13). Furthermore,
53
54 25 other urologic studies have observed a strong correlation between renal volume,
55
56
57
58
59
60

1
2
3 1 | calculated with enhanced and ~~unenhanced~~ enhanced CT, and renal function estimated with
4
5 2 | nuclear medicine renal scans (14). This methodology to assess the renal volume is a
6
7 3 | complex and resource-intensive procedure which requires expensive and complex
8
9 4 | software, an extensive learning curve, and time. These characteristics may render it
10
11 5 | impractical for use in a busy daily practice outside of investigational applications, and
12
13 6 | inaccessible in many resource-limited environments. The precision of the method
14
15 7 | used for renal volume assessment in this manuscript has been evaluated applying the
16
17 8 | equation developed by Isotani et al(15) et Shomiyama et al(10). These authors
18
19 9 | developed an equation to predict postoperative renal function after nephrectomy by
20
21 10 | renal volume change and they found a correlation between predicted and observed
22
23 11 | eGFR of 0.83. Applying this equation, our correlation between predicted and
24
25 12 | observed eGFR was 0.844, ($p < 0.000$), a result comparable with the already published
26
27 13 | literature. Thus, we believe that this process may produce a functional method to
28
29 14 | detect changes in kidney volume, which, if automated, could provide a predictive and
30
31 15 | automatic notification regarding renal malperfusion to clinicians who are mandated to
32
33 16 | survey patients following aortic aneurysm repair.
34
35
36
37
38
39
40
41
42
43
44
45
46
47
48
49
50
51
52
53
54
55
56
57
58
59
60

19 The relationship between vascular clinicians and advanced imaging has been evolving
20 over three decades. Isovoxel imaging and post processing software has made 3D
21 manipulation of anatomic images possible, and facilitated the use of complex
22 endovascular stent grafts for the repair of thoracoabdominal and juxtarenal
23 aneurysms. Advanced imaging techniques such as 3D fusion have been recently
24 introduced to operative procedures, the advent of hybrid operating theatres and fixed
25 imaging systems capable of performing cone-beam CT scans in the operative

1 environment. Use of advanced imaging has changed practice where available,
2 because it has been demonstrated to reduce radiation exposure and contrast utilization
3 in both EVAR and complex endovascular procedures (16)(17)(18). The potential
4 postoperative applications remain unexplored in either hardware or software based
5 systems. With the aim of extending fusion techniques during follow-up, we have
6 tested the accuracy of a fusion-based software to automatically calculate renal volume
7 during follow-up. Compared to the previously-tested semi-automated process, the
8 percentage of decrease in renal volume detected by the automatic fusion-based
9 software is reliable with an ICC of 0.877 ($p= 0.001$) at one year of follow-up for the
10 left kidney and 0.966 ($p<0.001$) for the right kidney. These data validate fusion-based
11 software as a reliable tool to automatically measure renal volume. In addition, in the
12 vast majority of our cases with renal occlusion the fusion-based automatic software
13 detected at least at 25% decrease in renal volume on the CT scan at moment of
14 detection when compared with the preoperative ~~one~~.

15
16 If a study of renal event rate in the published literature were undertaken, it would be
17 observed that renal artery angulation should play some role in the discussion of renal
18 volume loss. Renal artery angulation has been assessed in different studies to
19 determine their impact and correlation with renal function during follow-up (19) and
20 is hypothesized to be the cause of renal impairment after aneurysm repair. However,
21 despite careful analysis, even observed changes of renal artery angulation after
22 implantation of fenestrated and branched devices (4) have not been reliably associated
23 with renal impairment, ~~and are challenging to reproduce~~. The same results have been
24 published by Ou et al. (6), finding no relation between postoperative renal impairment
25 and the changes in the stent and vessel orientation, even if all the patients suffering

1
2
3 1 stent deformation presented renal impairment. This failure of correlation even
4
5 2 remains true when ~~haemodynamic~~hemodynamic outcomes are improved with caudal
6
7 3 orientation of renal stents(20). Thus, despite much suspicion that forced anatomic
8
9 4 changes may bear some culpability for the deterioration of renal function often seen
10
11 5 after aneurysm repair, contemporary imaging techniques have failed to provide proof.
12
13 6 We believe a functional indicator, such as renal volume, which links anatomic change
14
15 7 to important perfusion-related outcomes provides a surrogate measure of stent
16
17 8 performance, and may be a better indicator of the 4-dimensional behavior of the
18
19 9 stents. If automated, this could become a powerful and useful tool for clinicians who
20
21 10 have a busy aneurysm practice. Furthermore, the ability to detect ~~change~~ using an
22
23 11 imaging technique that does not involve contrast makes it more practical for use in
24
25 12 patients who have low grade renal impairment from any cause.
26
27
28
29
30

31 14 This study is a retrospective, pilot study to test the feasibility and accuracy of this
32
33 15 technique and thus included only a limited number of patients. Another limitation can
34
35 16 be consider the reproducibility of the semi-automated method, but it has been tested
36
37 17 applying the formula developed by Isotani et al(15) . Furthermore, the impact of
38
39 18 asymmetric changes in renal volume, as in the scenario where one of two accessories
40
41 19 renal arteries is embolized has not been fully assessed. More work is needed to make
42
43 20 this process fully automated and applicable to imaging processing platforms in all
44
45 21 jurisdictions.
46
47
48
49

50 23 **Conclusion**

51
52 24 This is the first report of a fusion-based algorithm to detect changes in renal volume
53
54 25 during postoperative surveillance using an automated process. Using this technique,
55
56
57
58
59
60

1 the standardised assessment of renal volume could be implemented with greater ease
2 and reproducibility in the current follow-up of endovascular procedures. Renal
3 volume has demonstrated to be a reliable marker of renal impairment.

4
5 **Conflict of Interest Disclosure:** TM Mastracci Research/Educational Support from
6 Cydar Medical; Consulting of Cook Medical. G Penney Co-funder/Employee of
7 Cydar Medical.

8
9 **BibliographyReferences**

- 10 1. Katsargyris A, Oikonomou K, Klonaris C, Töpel I, Verhoeven ELG. Comparison
11 of outcomes with open, fenestrated, and chimney graft repair of juxtarenal
12 aneurysms: are we ready for a paradigm shift? J Endovasc Ther Off J Int Soc
13 Endovasc Spec. 2013 Apr;20(2):159–69.
- 14 2. Verhoeven ELG, Katsargyris A, Bekkema F, Oikonomou K, Zeebregts CJ a. M,
15 Ritter W, et al. Editor’s Choice - Ten-year Experience with Endovascular Repair
16 of Thoracoabdominal Aortic Aneurysms: Results from 166 Consecutive Patients.
17 Eur J Vasc Endovasc Surg Off J Eur Soc Vasc Surg. 2015 May;49(5):524–31.
- 18 3. Kristmundsson T, Sonesson B, Dias N, Törnqvist P, Malina M, Resch T.
19 Outcomes of fenestrated endovascular repair of juxtarenal aortic aneurysm. J
20 Vasc Surg. 2014 Jan;59(1):115–20.
- 21 4. Martin-Gonzalez T, Pinçon C, Maurel B, Hertault A, Sobocinski J, Spear R, et al.
22 Renal Outcomes Following Fenestrated and Branched Endografting. Eur J Vasc
23 Endovasc Surg Off J Eur Soc Vasc Surg. 2015 May 25;

- 1
2
3 1 5. Mastracci TM, Eagleton MJ, Kuramochi Y, Bathurst S, Wolski K. Twelve-year
4
5 2 results of fenestrated endografts for juxtarenal and group IV thoracoabdominal
6
7 3 aneurysms. *J Vasc Surg.* 2015 Feb;61(2):355–64.
8
9
- 10 4 6. Ou J, Chan Y-C, Chan CY-T, Cheng SWK. Geometric Alteration of Renal
11
12 5 Arteries After Fenestrated Grafting and the Impact on Renal Function. *Ann Vasc*
13
14 6 *Surg.* 2017 Feb 24;
15
16
- 17 7 7. Heneghan RE, Starnes BW, Nathan DP, Zierler RE. Renal duplex ultrasound
18
19 8 findings in fenestrated endovascular aortic repair for juxtarenal aortic aneurysms.
20
21 9 *J Vasc Surg.* 2016 Apr;63(4):915–21.
22
23
- 24 10 8. Hertault A, Maurel B, Pontana F, Martin-Gonzalez T, Spear R, Sobocinski J, et al.
25
26 11 Benefits of Completion 3D Angiography Associated with Contrast Enhanced
27
28 12 Ultrasound to Assess Technical Success after EVAR. *Eur J Vasc Endovasc Surg*
29
30 13 *Off J Eur Soc Vasc Surg.* 2015 May;49(5):541–8.
31
32
33
- 34 14 9. Martin-Gonzalez T, Pinçon C, Hertault A, Maurel B, Labbé D, Spear R, et al.
35
36 15 Renal outcomes analysis after endovascular and open aortic aneurysm repair. *J*
37
38 16 *Vasc Surg.* 2015 Sep;62(3):569–77.
39
40
41
- 42 17 10. Shimoyama H, Isotani S, China T, Nagata M, Yokota I, Kitamura K, et al.
43
44 18 Automated renal cortical volume measurement for assessment of renal function in
45
46 19 patients undergoing radical nephrectomy. *Clin Exp Nephrol.* 2017 Apr 10;
47
48
- 49 20 11. Yushkevich PA, Piven J, Hazlett HC, Smith RG, Ho S, Gee JC, et al. User-guided
50
51 21 3D active contour segmentation of anatomical structures: significantly improved
52
53 22 efficiency and reliability. *NeuroImage.* 2006 Jul 1;31(3):1116–28.
54
55
56
57
58
59
60

- 1
2
3 12. Yano M, Lin MF, Hoffman KA, Vijayan A, Pilgram TK, Narra VR. Renal
4
5 2 measurements on CT angiograms: correlation with graft function at living donor
6
7 3 renal transplantation. *Radiology*. 2012 Oct;265(1):151–7.
- 8
9
10 4 13. Herts BR, Sharma N, Lieber M, Freire M, Goldfarb DA, Poggio ED. Estimating
11
12 5 glomerular filtration rate in kidney donors: a model constructed with renal volume
13
14 6 measurements from donor CT scans. *Radiology*. 2009 Jul;252(1):109–16.
- 15
16
17 7 14. Morrisroe SN, Su RR, Bae KT, Eisner BH, Hong C, Lahey S, et al. Differential
18
19 8 renal function estimation using computerized tomography based renal
20
21 9 parenchymal volume measurement. *J Urol*. 2010 Jun;183(6):2289–93.
- 22
23
24
25 10 15. Isotani S, Shimoyama H, Yokota I, Noma Y, Kitamura K, China T, et al. Novel
26
27 11 prediction model of renal function after nephrectomy from automated renal
28
29 12 volumetry with preoperative multidetector computed tomography (MDCT). *Clin*
30
31 13 *Exp Nephrol*. 2015 Oct;19(5):974–81.
- 32
33
34
35 14 16. Hertault A, Maurel B, Sobocinski J, Martin Gonzalez T, Le Roux M, Azzaoui R,
36
37 15 et al. Impact of hybrid rooms with image fusion on radiation exposure during
38
39 16 endovascular aortic repair. *Eur J Vasc Endovasc Surg Off J Eur Soc Vasc Surg*.
40
41 17 2014 Oct;48(4):382–90.
- 42
43
44 18 17. Dijkstra ML, Eagleton MJ, Greenberg RK, Mastracci T, Hernandez A.
45
46 19 Intraoperative C-arm cone-beam computed tomography in fenestrated/branched
47
48 20 aortic endografting. *J Vasc Surg*. 2011 Mar;53(3):583–90.
- 49
50
51 21 18. Tacher V, Lin M, Desgranges P, Deux J-F, Grünhagen T, Becquemin J-P, et al.
52
53 22 Image guidance for endovascular repair of complex aortic aneurysms: comparison

1
2
3 1 of two-dimensional and three-dimensional angiography and image fusion. *J Vasc*
4
5 2 *Interv Radiol JVIR*. 2013 Nov;24(11):1698–706.

6
7
8 3 19. Conway BD, Greenberg RK, Mastracci TM, Hernandez AV, Coscas R. Renal
9
10 4 artery implantation angles in thoracoabdominal aneurysms and their implications
11
12 5 in the era of branched endografts. *J Endovasc Ther Off J Int Soc Endovasc Spec*.
13
14 6 2010 Jun;17(3):380–7.

15
16
17 7 20. Ou J, Tang AYS, Chiu TL, Chow KW, Chan YC, Cheng SWK. Haemodynamic
18
19 8 Variations of Flow to Renal Arteries in Custom-Made and Pivot Branch
20
21 9 Fenestrated Endografting. *Eur J Vasc Endovasc Surg Off J Eur Soc Vasc Surg*.
22
23 10 2017 Jan;53(1):133–9.

24
25
26
27 11

28
29
30 12

31
32 13

33
34 14

35
36 15

37
38 16

39
40 17

41
42 18
43
44
45
46
47
48
49
50
51
52
53
54
55
56
57
58
59
60

FIGURES LEGENDS

Figure 1. Renal volume calculated with the semiautomated software. **a.** 3D VR reconstruction of the kidney selected. **b.** MPR view of the kidney selection. **c.** Renal contour in an axial view. **d.** Estimation renal volume

Figure 2. Renal volume calculated with the new fusion-based automatic software. **a.** Manually selection points in the preoperative CT **b.** Manually pick kidney centre in the postoperative CT scan. The kidneys are then represented in orthogonal views on post processing software so their three dimensional volume can be assessed **c.** Preoperative kidney volume. **d.** Postoperative kidney positioned and scaled, needing to be enlarged by 81% to accurately fuse with preoperative kidney

Figure 3. Correlation between predicted eGFR, based on renal volume calculated with the semiautomated process, and observed eGFR

~~**Figure 4.** Correlation between the semiautomated process and the new fusion-based automatic software for the right kidney at 1 year follow up~~

Demographic characteristics	Non occlusion group	Occlusion group
Age at procedure (years) (median, range)	70.50 [65.25-81.50]	71.50 [65.25-78.25]
BMI (kg/m ²) (median, range)	29.8 [22.6-35.1]	22.8 [21.5-26.3]
Sex (%)		
<i>Male</i>	87.5 (n=7)	87.5 (n=7)
<i>Female</i>	12.5 (n=1)	12.5 (n=1)
Hypertension (%)	75 (n=6)	83.3 (n=5)
Dyslipidaemia (%)	75 (n=6)	100 (n=6)
COPD (%)	50 (n=4)	100 (n=6)
Smoking (%)		
<i>Yes</i>	0 (n=0)	33.3 (n=2)
<i>No</i>	25 (n=2)	50 (n=3)
<i>Former</i>	75 (n=6)	16.7 (n=1)
Diabetes (%)	25 (n=2)	16.7 (n=1)
Ischaemic heart disease (%)	62.5 (n=5)	50 (n=3)
Chronic kidney disease (eGFR<60 ml/min) (%)	25 (n=2)	66.7 (n=4)
Aneurysm size (mm) (median, range)	61 [56-72]	68 [61-75]
Preoperative renal function (ml/min) (median, range)	80.5 [49.25-89.75]	55 [42.25-74.50]

BMI: Body Mass Index; COPD: Chronic Obstructive Pulmonary Disease; eGFR: estimated Glomerular Filtration Rate

Table 1. Demographic characteristics divided by groups.

Patient number	Renal artery occluded	Time occlusion	% Decrease renal volume
1	Left	1 year follow up	61
2	Left	1 month follow up	29
3	Left	1 year follow up	16
4	Left	1 month follow up	13
5	Right	1 year follow up	49
	Left	1 year follow up	23
6	Right	1 month follow up	35
7	Right	1 year follow up	74
8	Left	1 month follow up	19

Table 2. % Decrease in renal volume detected by the automatic method at the moment of renal artery occlusion.

1
2
3
4
5
6
7
8
9
10
11
12
13
14
15
16
17
18
19
20
21
22
23
24
25
26
27
28
29
30
31
32
33
34
35
36
37
38
39
40
41
42
43
44
45
46
47
48
49
50
51
52
53
54
55
56
57
58
59
60



Figure 1A

286x280mm (300 x 300 DPI)

1
2
3
4
5
6
7
8
9
10
11
12
13
14
15
16
17
18
19
20
21
22
23
24
25
26
27
28
29
30
31
32
33
34
35
36
37
38
39
40
41
42
43
44
45
46
47
48
49
50
51
52
53
54
55
56
57
58
59
60



Figure 1B

286x278mm (300 x 300 DPI)

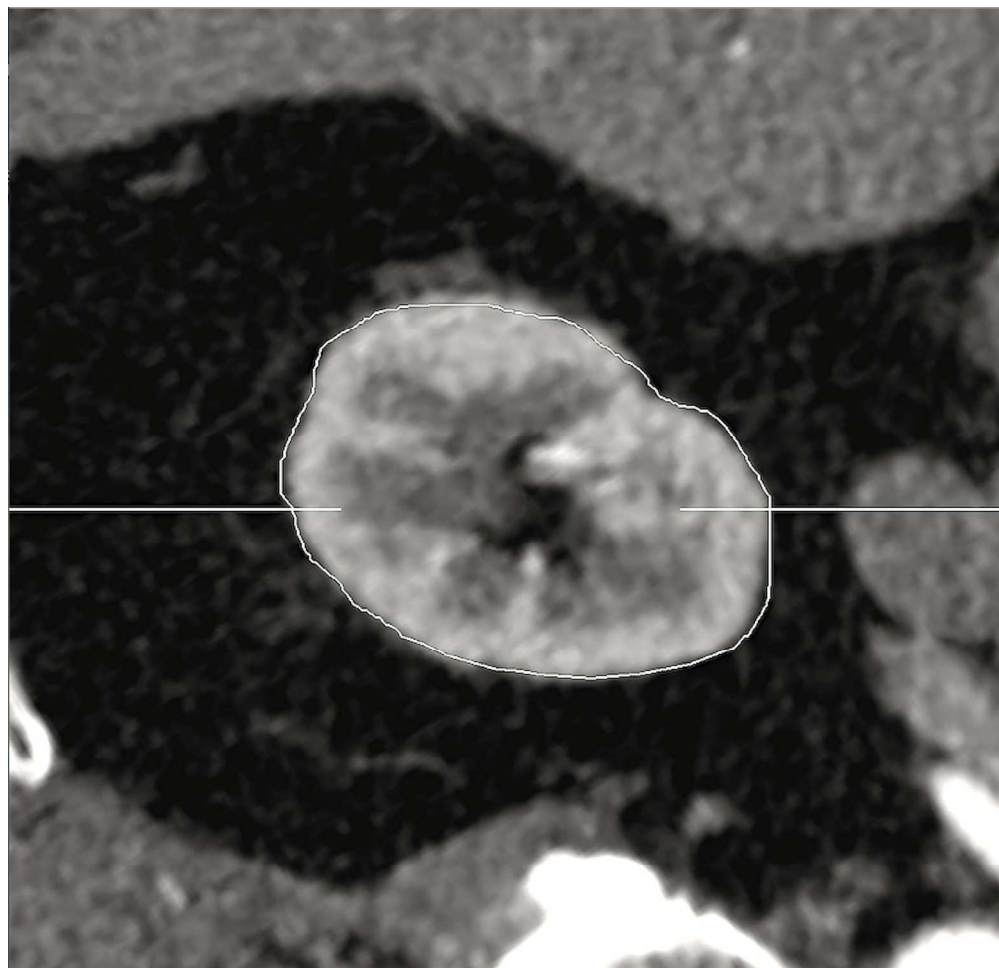


Figure 1C

286x275mm (300 x 300 DPI)

1
2
3
4
5
6
7
8
9
10
11
12
13
14
15
16
17
18
19
20
21
22
23
24
25
26
27
28
29
30
31
32
33
34
35
36
37
38
39
40
41
42
43
44
45
46
47
48
49
50
51
52
53
54
55
56
57
58
59
60

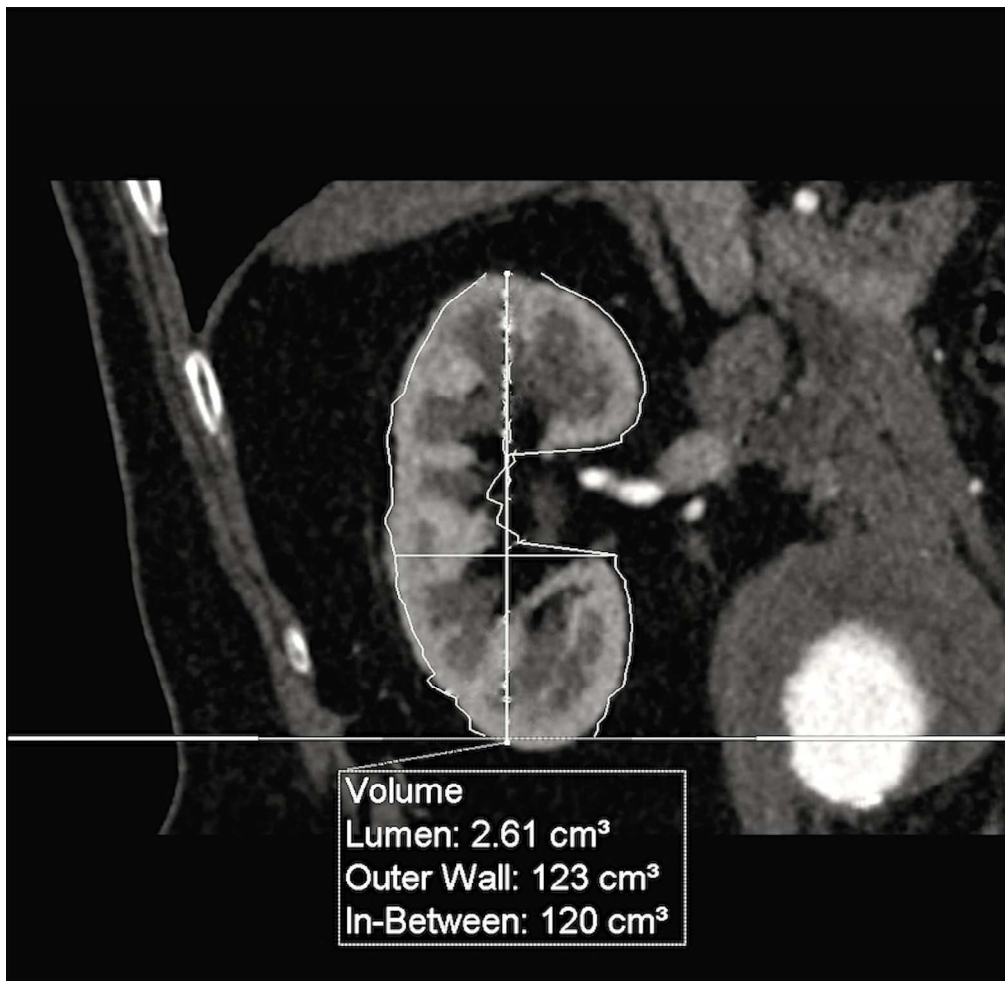


Figure 1D

284x276mm (300 x 300 DPI)

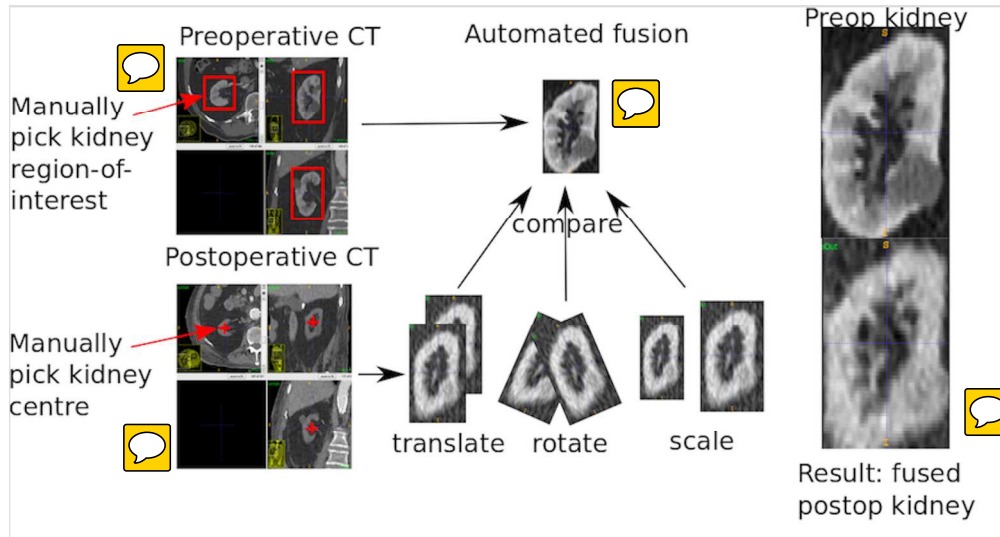


Figure 2

314x167mm (300 x 300 DPI)

1
2
3
4
5
6
7
8
9
10
11
12
13
14
15
16
17
18
19
20
21
22
23
24
25
26
27
28
29
30
31
32
33
34
35
36
37
38
39
40
41
42
43
44
45
46
47
48
49
50
51
52
53
54
55
56
57
58
59
60

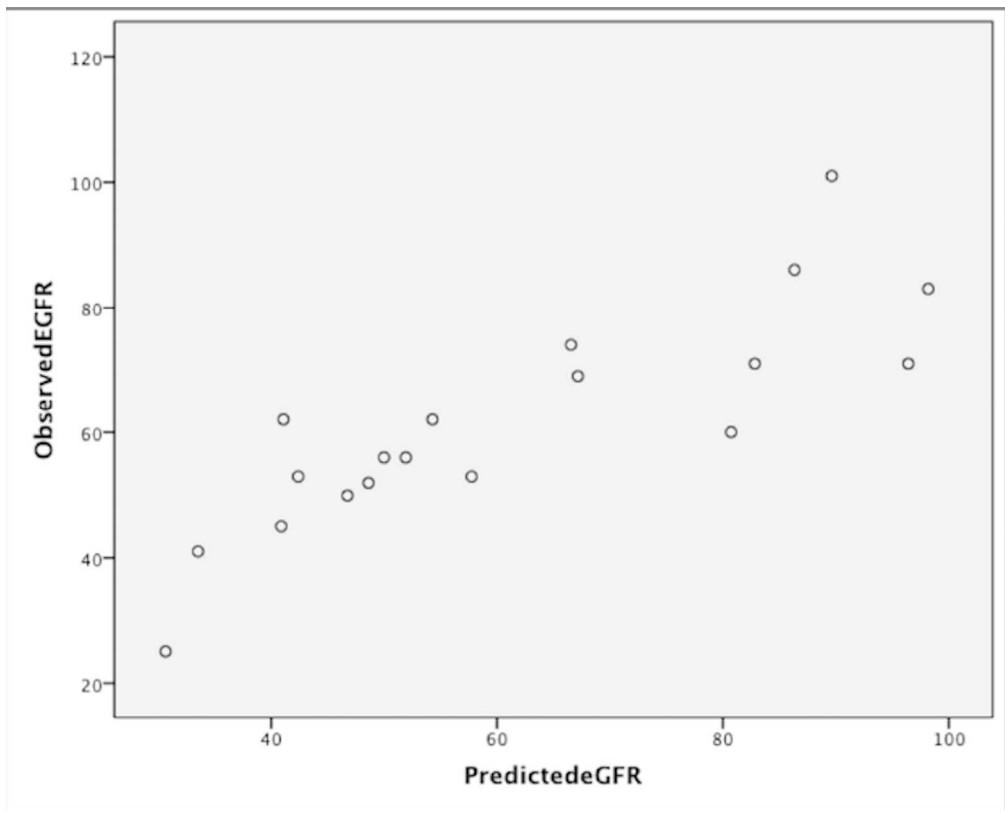


Figure 3

218x175mm (300 x 300 DPI)